

# Scattering Phase of Quantum Dots: Emergence of Universal Behavior

Rafael A. Molina,<sup>1</sup> Rodolfo A. Jalabert,<sup>2</sup> Dietmar Weinmann,<sup>2</sup> and Philippe Jacquod<sup>3,4</sup>

<sup>1</sup>*Instituto de Estructura de la Materia, CSIC, Serrano 123, 28006 Madrid, Spain*

<sup>2</sup>*Institut de Physique et Chimie des Matériaux de Strasbourg, UMR 7504, CNRS-UdS,  
23 rue du Loess, BP 43, 67034 Strasbourg Cedex 2, France*

<sup>3</sup>*Physics Department, University of Arizona, 1118 E. Fourth Street, P.O. Box 210081, Tucson, Arizona 85721, USA*

<sup>4</sup>*Département de Physique Théorique, Université de Genève, CH-1211 Genève 4, Switzerland*

(Received 5 August 2011; published 13 February 2012)

We investigate scattering through chaotic ballistic quantum dots in the Coulomb-blockade regime. Focusing on the scattering phase, we show that large universal sequences emerge in the short wavelength limit, where phase lapses of  $\pi$  systematically occur between two consecutive resonances. Our results are corroborated by numerics and are in qualitative agreement with existing experiments.

DOI: [10.1103/PhysRevLett.108.076803](https://doi.org/10.1103/PhysRevLett.108.076803)

PACS numbers: 73.23.Hk, 03.65.Vf, 73.50.Bk, 85.35.Ds

Quantum mechanics fundamentally differs from classical mechanics in that time evolutions are determined by complex probability amplitudes instead of real probabilities. The associated phase is a key element to understand mesoscopic transport experiments on Aharonov-Bohm (AB) conductance oscillations, weak localization, and conductance fluctuations [1]. However, these transport measurements, like any other measurement, do not directly measure scattering phases. In their phase-sensitive experiment, Yacoby *et al.* pioneered an entirely new field of mesoscopic physics, by embedding a ballistic quantum dot (QD) in one arm of an AB interferometer [2]. The sustained interest in these and following [3–5] experiments, that persists until today, relies on the difficulty to consistently and generically explain these measurements.

When a QD in the Coulomb-blockade (CB) regime is placed in one arm of a mesoscopic ring threaded by a flux  $\phi$  (see the inset in Fig. 1), the conductance through the ring reads [6,7]

$$g = g_0 + \sum_n g_n \cos(2\pi n \phi / \phi_0 + \beta_n), \quad (1)$$

with the quantum of flux  $\phi_0$ . Measuring the lowest harmonics of the AB oscillations in  $\phi$  allows one to extract the phase  $\beta_1$  as a function of a gate voltage  $V_g$  applied to the QD. Under suitable conditions,  $\beta_1$  can be related to the scattering phase of the QD [7]. A multiterminal configuration is required in order to get a one-to-one relationship between the two phases, while in a two-terminal setup  $\beta_1$  can take only the values 0 or  $\pi$  [3,6]. In the multiterminal case, a gradual increase of  $\pi$  in the transmission phase is obtained as a function of the gate voltage for every CB peak, in agreement with the Friedel sum rule [8–10]. Abrupt lapses of  $\pi$  occur between resonances in both configurations at values of  $V_g$  for which the transmission amplitude of the QD is so small that the AB oscillations are below the experimental visibility threshold. For relatively large QD with a few hundred electrons [2,3], the lapses

were seen to appear systematically between every consecutive pair of resonances. This surprising behavior, termed universal, is observed in two- or multiterminal configurations. Smaller dots were more recently investigated, where the number of electrons was tuned from about 20 down to zero [5]. A crossover from the universal regime, where successive peaks are in phase, to a mesoscopic regime, where phase lapses occur in a random fashion, was observed when decreasing the number of electrons in the QD by the action of  $V_g$ . Multiterminal configurations with one QD in each arm of the AB interferometer have also been investigated [4], which determined the important role of the magnetic field in the phase lapses. The understanding of the crossover from the mesoscopic to the universal

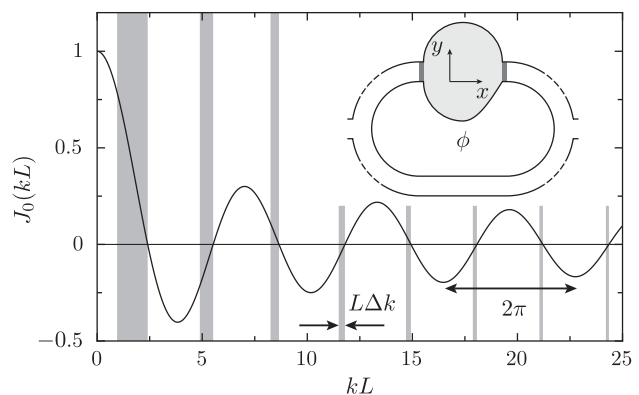


FIG. 1. 0th order Bessel function  $J_0(kL)$ . The shaded areas indicate regions where  $\bar{D}_n$  is negative. For two-dimensional systems, the width of these intervals, and the probability of not obtaining a phase lapse between two resonances, decreases as  $L\Delta k \sim (kL)^{-1}$ . Inset: Aharonov-Bohm interferometer, threaded by a flux  $\phi$ , with an asymmetric dot (shaded) tunnel-embedded in its upper arm. The distance between the entrance and exit points of the dot is  $L$ . The dashed lines on the arms of the interferometer stand for any number of potential additional leads.

regime and the role of the symmetries are the main goals of our work.

For a lateral QD in the CB regime, a single lead channel dominantly couples to the QD, and transport through the QD is characterized by a  $2 \times 2$  scattering matrix:

$$S = \begin{pmatrix} r & t' \\ t & r' \end{pmatrix} = e^{i\alpha} \begin{pmatrix} ie^{i\xi} \cos\theta & e^{i\eta} \sin\theta \\ e^{-i\eta} \sin\theta & ie^{-i\xi} \cos\theta \end{pmatrix}. \quad (2)$$

We note  $t$  ( $t'$ ) and  $r$  ( $r'$ ) the transmission and reflection amplitudes, respectively, for particles coming from the left (right) of the QD. The angle  $\theta$  is restricted to the interval  $[0, \pi)$ , while the phases  $\alpha$ ,  $\eta$ , and  $\xi$  are defined on  $[0, 2\pi)$ . The scattering phase  $\alpha$  is related to the density of states of the QD through the Friedel sum rule [6,8–10]. When considering the phase evolution as a function of an external parameter (like  $V_g$ ), it is convenient to work with the accumulated phase  $\alpha_c$ , whose range of definition is not restricted to the interval  $[0, 2\pi)$ .

Equation (2) represents the most general  $2 \times 2$  unitary matrix. When time-reversal invariance is present, one has  $\eta = 0$  or  $\pi$ . Right-left parity symmetry would restrict  $\xi$  to either 0 or  $\pi$ . Here, we consider generic QDs with arbitrary  $\xi$ . When the many-body problem is considered in its full complexity,  $S$  represents an effective one-particle scattering matrix that can be obtained, for instance, through the embedding method [11,12]. If we restrict the description of the many-body problem to the constant-interaction model (CIM), the CB phenomena can be interpreted in terms of single-particle quantities [13], and, close to resonances,  $S$  is given by the transmission and reflection amplitudes of single-particle states in a mean-field potential. When the underlying classical scattering is chaotic,  $S$  has well-defined statistical properties determined by the symmetries of the problem only [14]. In structures with time-reversal symmetry,  $t = e^{i\alpha} \sin\theta$ , and, even if  $t$  is a complex continuous function of the real variable  $V_g$ , the phase  $\alpha$  exhibits a phase lapse of  $\pi$  whenever  $t$  vanishes.

Within the CIM and in the absence of a magnetic field, the one-particle wave functions can be chosen to be real. With the exception of peculiar cases with very different values of the resonance widths between consecutive resonances, a zero of the transmission generically appears between two successive resonances depending on the sign of [10]

$$D_n = \gamma_n^l \gamma_n^r \gamma_{n+1}^l \gamma_{n+1}^r. \quad (3)$$

The partial-width amplitude (or effective coupling) of the eigenstate  $\psi_n$  of the QD is given by [13]

$$\gamma_n^{l(r)} = \left( \frac{\hbar^2 k P_c}{m} \right)^{1/2} \int_0^W dy \Phi_{l(r)}(y) \psi_n(x^{l(r)}, y). \quad (4)$$

Here,  $\Phi_{l(r)}$  is the first transversal subband wave function in the left (right) lead of width  $W$ , the integration is along the transverse coordinate  $y$  at the entrance or exit of the QD

located at  $x = x^{l(r)}$ ,  $P_c$  is the transparency of the tunnel barriers,  $k$  is the Fermi wave vector in the leads, and  $m$  is the electron mass. In lattice models with one-dimensional leads [7,10], the two partial-width amplitudes are simply proportional to the value of the wave function at the extreme point connecting the QD to the corresponding lead.

We call  $\gamma_n^l \gamma_n^r$  the *parity* of the  $n$ th resonance [10]. When  $D_n > 0$  [equal parity of the  $n$ th and  $(n+1)$ st resonances] there is one zero (or an odd number of zeros) between the  $n$ th and  $(n+1)$ st resonances, while for  $D_n < 0$  (opposite parities) there is no zero (or an even number of zeros) between the two resonances. For one-dimensional scatterers,  $D_n$  is always negative, which results in the absence of transmission zeros reflecting the impossibility of obtaining destructive interfering paths in one dimension [8]. Numerical simulations on two-dimensional disordered lattice systems, on the other hand, yield an equal probability for positive or negative  $D_n$  [10], which is at odds with the experimental observation of a universal regime with zeros between any two consecutive resonances. Several theoretical refinements have been proposed to solve the puzzle [10,15–22], where specific geometries or effective couplings, or extensions of the CIM are considered.

The latter path is, in principle, the most natural one and was actually already suggested in Ref. [2]. However, the small sizes that can be handled within a full many-body description make the universal regime hardly reachable. Moreover, even if the influence of electron-electron interaction can be spotted in some circumstances [11,20,22], the corresponding results are not generic. On the other hand, the CIM gives an excellent description of the statistical distribution of the height of the CB peaks [13,23], which is determined by the one-particle widths  $\gamma_n^{l,r}$ . It is then expected that the statistics of the resonance parities and consequently of the transmission zeros are within the reach of the CIM. Below, assuming that this is the case, we incorporate well-known correlations of quantum chaotic wave functions in our analysis of  $D_n$ . In this way, we account for the transition from a mesoscopic to a universal regime.

Long-range wave-function correlations in quantum chaotic systems were first pointed out by Berry [24], who suggested to model the wave functions as random superpositions of plane waves with fixed energy  $\hbar^2 k^2 / (2m)$ . For a two-dimensional chaotic billiard with eigenfunctions  $\psi_n$ , this gives the wave-function correlator

$$\overline{\psi_n(\mathbf{r}) \psi_n(\mathbf{r}')} = J_0(k|\mathbf{r} - \mathbf{r}'|) / \mathcal{A}. \quad (5)$$

The bar stands for a local average,  $\mathcal{A}$  is the area of the billiard, and  $J_0$  is the 0th Bessel function of the first kind. Corrections to Eq. (5) appear in confined systems when the observation points approach the boundaries [25], which is the case we are interested in. For  $\mathbf{r} \neq \mathbf{r}'$ , these corrections are, however, small, and we will neglect them. Equation (5)

has been successfully used to explain the long-range (in energy) modulation of the peak-height distribution in the CB regime [26].

If we call  $L$  the distance from the entrance to the exit of the QD and assume that successive eigenfunctions are uncorrelated, we have for the case  $W \ll L$  of relevance for us

$$\bar{D}_n \sim J_0(k_n L) J_0(k_{n+1} L). \quad (6)$$

Taking  $L$  as the typical linear dimension of the QD, we have  $k_{n+1} - k_n \simeq \Delta k = \pi/(kL^2)$ . Thus,  $\bar{D}_n$  is negative when the Bessel functions in Eq. (6) have different signs, which happens only if  $kL$  falls in an interval of length  $L\Delta k$  before one zero of  $J_0(kL)$ . This is sketched in Fig. 1. In the semiclassical limit  $kL \gg 1$ , we have  $J_0(kL) \sim \sqrt{2/(\pi kL)} \cos(kL - \pi/4)$ , and therefore the probability  $\mathcal{P}$  of obtaining a negative  $\bar{D}_n$  can be estimated as the ratio of  $2L\Delta k$  over the period  $2\pi$ , that is,

$$\mathcal{P} \sim \frac{1}{kL}. \quad (7)$$

This simple analysis explains why when the dot is progressively filled the equal-parity case ( $\bar{D}_n > 0$ ) results with probability approaching one. Moreover, it also shows that the sequence of peaks and zeros appears over intervals in  $kL$  that are of length  $\pi$ , containing a number  $kL$  of resonances. The sole assumption that wave functions have quantum chaotic correlations thus predicts the emergence of large universal sequences of resonances and transmission zeros. This is our main result.

In order to illustrate and test our analytical prediction, we have performed numerical calculations of the transmission amplitude of spinless electrons through a non-interacting QD with the shape of a desymmetrized stadium billiard, where one of the quarter circles is replaced by a cosine curve. This is sketched in the inset in Fig. 1. The QD is connected to leads through tunnel barriers as in Ref. [23]. The parameter of variation is the gate voltage  $V_g$ , which induces changes in the wave vector  $k$  within the QD. Phase increases of  $\pi$  are correlated with transmission peaks, while phase lapses of  $\pi$  are assigned at the values of  $V_g$  where the transmission vanishes. We show in Fig. 2 a sequence of eight resonances for 174–182 electrons on the dot, similar to the experiments of Refs. [2,3]. This sequence exhibits a perfect alternation of resonances and zeros. We found that this is the generic behavior for  $kL > 10$ .

We next present in Fig. 3 (thick lines) the accumulated scattering phase  $\alpha_c^{(-)}$  (the superscript indicates that we follow the convention used in the experiments of taking all phase lapses as  $-\pi$ ), together with the number of accumulated resonances (zeros)  $N_{r(z)}$ .  $N_r$  and  $N_z$  grow with almost the same mean rate for  $kL > 10$  (at least up to the maximum values of  $kL \simeq 100$  that we used). In the inset, we show the probability  $\mathcal{P} = (\Delta N_r - \Delta N_z)/\Delta N_r$  of obtaining more resonances than transmission zeros in an

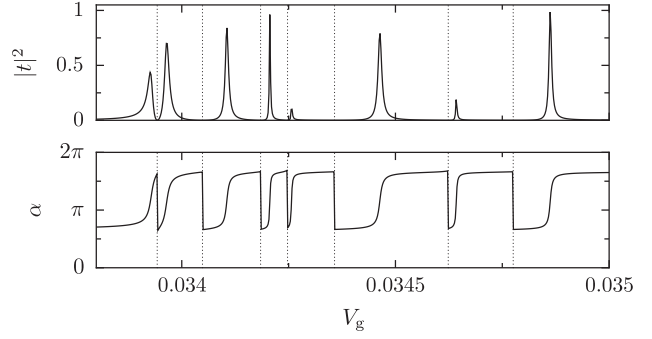


FIG. 2. Transmission  $|t|^2$  and scattering phase  $\alpha$  as a function of the applied gate voltage  $V_g$ . The number of electrons in the dot varies between 174 and 182. Smooth increases of  $\pi$  in  $\alpha$  obtained for each resonance alternate with phase lapses of  $-\pi$  when the transmission vanishes (dotted vertical lines).

interval of  $V_g$ .  $\mathcal{P}$  is proportional to the difference of slopes  $\Delta N_r/\Delta V_g - \Delta N_z/\Delta V_g$ . In agreement with the theoretical analysis, the regions where there are no zeros between resonances show up with a periodicity (in  $kL$ ) of approximately  $\pi$  and are separated by intervals where there is an alternation of peaks and zeros. Upon increasing  $k$ , sequences exhibiting perfectly alternating resonances and zeros become larger and larger, favoring the observation of the universal behavior.

The importance of a magnetic field in the phase-sensitive measurements has been underlined in experimental [4] and theoretical [8,27] works. Once we have a magnetic field breaking time-reversal symmetry, the wave functions are no longer real,  $D_n$  becomes complex,

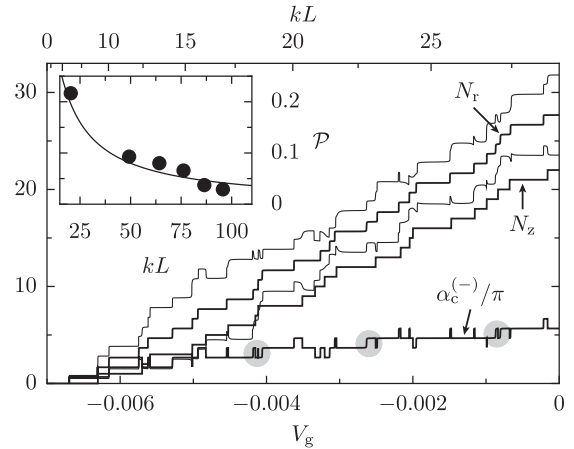


FIG. 3. Thick lines: Accumulated scattering phase  $\alpha_c^{(-)}/\pi$  and number of resonances (zeros)  $N_{r(z)}$  as a function of  $V_g$  (or  $kL$ ). The shaded spots indicate the regions where  $N_z$  lags  $N_r$ . They are separated approximately by  $\pi$  in  $kL$ . Thin lines:  $\alpha_c/\pi$  for a small positive and negative magnetic field. Inset:  $\mathcal{P} = (\Delta N_r - \Delta N_z)/\Delta N_r$  taken at various intervals of  $V_g$  as a function of  $kL$ . The line is a guide to the eye that decreases as  $(kL)^{-1}$ , showing the good agreement of the numerical calculations with the prediction of Eq. (7).



and our analysis in terms of the parity of the resonances is no longer applicable. We included a magnetic field in our numerical calculations, using a desymmetrized structure in order to truly break time-reversal symmetry [28]. We observed that the exact transmission zeros obtained at  $B = 0$  become minima with small (but finite) values. Such a behavior is expected, since a monochannel QD has divergent probability of exhibiting a vanishing  $|t|$  when  $B = 0$ , while the transmission distribution is uniform in the interval  $(0, 1)$  for the case where time-reversal symmetry is completely broken [13,14,23].

Avoiding transmission zeros in the complex plane eliminates the  $\pi$  phase lapses in favor of continuous jumps with large (but finite) derivatives and magnitude  $\lesssim \pi$ . At finite fields, the ambiguity in the definition of the accumulated phase  $\alpha_c$  is then lifted. In Fig. 3, we present  $\alpha_c$  for a very small positive (negative) field (thin lines). The phase jumps for small positive fields are opposite to those for negative fields, and the difference in the accumulated phases is of statistical nature (of the order of the square root of the number of avoided zeros), illustrating the diffusion away from the origin in the complex plane for small  $B$  fields. On the other hand, the mean slope of the accumulated phase is the same in both cases and coincides with the slope of  $\pi N_r$ . We point out that the difference between the Friedel and transmission phases [8,9] arises from the ambiguity in the definition of  $\alpha_c$  at  $B = 0$ . This ambiguity is lifted if we define  $\alpha_c(B = 0) = \lim_{B \rightarrow 0^+} \alpha_c(B)$ .

Experimentally, the visibility threshold for the AB oscillations can make the continuous phase evolution at small fields indistinguishable from the phase lapses at  $B = 0$ . Breaking time-reversal symmetry reduces the probability of obtaining very small transmission values and thereby favors the observation of a continuous phase evolution as a function of  $V_g$ . The magnetic field needed for breaking time-reversal symmetry in the QD scales as  $k^{-1/2}$  [13,23]. Experimentally, larger fields have been used in Ref. [2], where, however, abrupt phase lapses  $\pi$  are enforced by the use of a two-terminal setup. References [3,5], on the other hand, used fields too weak to break time-reversal symmetry. Reference [4] reported phase lapses, and thus universal behavior, in specific magnetic field ranges only, where, presumably, the transmission drops below the experimental visibility threshold and is thus indistinguishable from a true zero. We predict that, under the experimental conditions of Refs. [3,5], a magnetic field of the order of 500G will eliminate some of the phase lapses observed at weak fields.

Another test would be to investigate diffusive QDs. In a two-dimensional system with short-range disorder characterized by an elastic mean-free path  $\ell \ll L$ , the right-hand side of Eq. (5) is suppressed by an exponentially small prefactor  $e^{-L/2\ell}$ . When there is a sufficient amount of disorder, one obtains  $\mathcal{P} = 1/2$ , as in Ref. [10], and thus the universal regime disappears. The experiments report values  $\ell \simeq 5\text{--}15 \mu\text{m}$  [2–5] with QDs of submicron sizes,

well in the ballistic regime. We predict that a larger, more disordered QD would exhibit a mesoscopic regime with phase lapses randomly distributed between consecutive resonances with a probability  $\mathcal{P} = 1/2$ . We also note that the weaker screening of impurities in few-electron QDs makes the dots less ballistic, favoring the observation of the mesoscopic regime.

Up to now, we have ignored the effects of the electronic spin. The first such effect is a trivial factor of 2 in the density of states that affects the relation between  $k$  and  $N$ . Second, within the CIM the filling of spin-degenerate one-particle states is by pairs [13]. We note that this spin degeneracy would divide by two the probability of obtaining, in our analytical and numerical approaches, consecutive resonances without a phase lapse and, hence, favor the universal behavior. Correlation effects may not be negligible in Coulomb-blockade valleys, but they are not expected to significantly alter the transmission phases close to the resonances nor the occurrence of phase lapses in between.

Our single-particle theory for ballistic QDs thus predicts the emergence of a universal behavior of scattering phases at large  $kL$ . Our numerics indicate that this crossover occurs around  $kL \simeq 10$ , which, for two-dimensional structures, corresponds to putting  $\sim 15$  electrons on the dot. This is qualitatively in agreement with the crossover reported in Ref. [5] and with the universal behavior reported in Refs. [2,3], which work in the range  $kL \gtrsim 50$ . We note that another condition is that  $kL$  is large enough that the wave functions resolve the chaoticity of the cavity, which also usually occurs around  $kL \simeq 10$ . We predict the disappearance of the observed universal regime (i) in the presence of a large magnetic field and (ii) in larger, more disordered dots in the diffusive regime. These predictions could be the basis for a comparison with alternative theories, like the one of Ref. [20].

In conclusion, we have provided quantitative, checkable predictions for the probability of observing long sequences of alternating transmission zeros and resonances in scattering through quantum dots, which are consistent with the experiments of Refs. [2–5]. We stress the probabilistic character of our findings and, in particular, that the absence of phase lapses between resonances is always possible. We hope that this will stimulate new experimental investigations.

We thank P. Schmitteckert for useful discussions. We acknowledge support from the Spanish MICINN through Project No. FIS2009-07277, the NSF under Grant No. DMR-0706319, and the ANR through Grant No. ANR-08-BLAN-0030-02.

- 
- [1] Y. Imry, *Introduction to Mesoscopic Systems* (Oxford University Press, Oxford, 2002), 2nd ed.
  - [2] A. Yacoby *et al.*, *Phys. Rev. Lett.* **74**, 4047 (1995).
  - [3] R. Schuster *et al.*, *Nature (London)* **385**, 417 (1997).

- [4] M. Sigrist *et al.*, *Phys. Rev. Lett.* **93**, 066802 (2004).
- [5] M. Avinun-Kalish *et al.*, *Nature (London)* **436**, 529 (2005).
- [6] A. Levy Yeyati and M. Büttiker, *Phys. Rev. B* **52**, R14360 (1995).
- [7] A. Aharony *et al.*, *Phys. Rev. B* **66**, 115311 (2002).
- [8] H.-W. Lee, *Phys. Rev. Lett.* **82**, 2358 (1999).
- [9] T. Taniguchi and M. Büttiker, *Phys. Rev. B* **60**, 13814 (1999).
- [10] A. Levy Yeyati and M. Büttiker, *Phys. Rev. B* **62**, 7307 (2000).
- [11] R. A. Molina *et al.*, [arXiv:1202.1253](#) [J. Phys. Conf. Ser. (to be published)].
- [12] R. A. Molina *et al.*, *Phys. Rev. B* **67**, 235306 (2003).
- [13] Y. Alhassid, *Rev. Mod. Phys.* **72**, 895 (2000).
- [14] R. A. Jalabert, J.-L. Pichard, and C. W. J. Beenakker, *Europhys. Lett.* **27**, 255 (1994); H. Baranger and P. Mello, *Phys. Rev. Lett.* **73**, 142 (1994); R. A. Jalabert and J.-L. Pichard, *J. Phys. I (France)* **5**, 287 (1995).
- [15] G. Hackenbroich, *Phys. Rep.* **343**, 463 (2001).
- [16] R. Baltin and Y. Gefen, *Phys. Rev. Lett.* **83**, 5094 (1999).
- [17] P. G. Silvestrov and Y. Imry, *Phys. Rev. Lett.* **85**, 2565 (2000).
- [18] D. I. Golosov and Y. Gefen, *Phys. Rev. B* **74**, 205316 (2006).
- [19] A. Bertoni and G. Goldoni, *Phys. Rev. B* **75**, 235318 (2007).
- [20] C. Karrasch *et al.*, *Phys. Rev. Lett.* **98**, 186802 (2007).
- [21] M. Goldstein *et al.*, *Phys. Rev. B* **79**, 125307 (2009).
- [22] J. P. Bergfield, Ph. Jacquod, and C. A. Stafford, *Phys. Rev. B* **82**, 205405 (2010).
- [23] R. A. Jalabert, A. D. Stone, and Y. Alhassid, *Phys. Rev. Lett.* **68**, 3468 (1992).
- [24] M. V. Berry, *J. Phys. A* **10**, 2083 (1977).
- [25] J. D. Urbina and K. Richter, *Phys. Rev. E* **70**, 015201(R) (2004).
- [26] E. E. Narimanov *et al.*, *Phys. Rev. B* **64**, 235329 (2001).
- [27] T.-S. Kim *et al.*, *Phys. Rev. B* **65**, 245307 (2002).
- [28] M. Robnik and M. V. Berry, *J. Phys. A* **18**, 1361 (1985).